In-vivo exposure of a plant model organism for the assessment of the ability of PM samples to induce oxidative stress

Emanuele Vaccarella [a], Diego Piacentini [a], Giuseppina Falasca [a], Silvia Canepari [a,b], Lorenzo Massimi [a,b,*]

[a] Department of Environmental Biology, Sapienza University of Rome, P. le Aldo Moro, 5, Rome 00185, Italy
[b] C.N.R. Institute of Atmospheric Pollution Research, Via Salaria, Km 29,300, Monterotondo St., Rome 00015, Italy

ARTICLE INFO

ABSTRACT

This study aims to propose an innovative, simple, rapid, and cost-effective method to study oxidative stress induced by PM through in-vivo exposure of the plant model organism *Arabidopsis thaliana*. *A. thaliana* seedlings were exposed to urban dust certified for its elemental content and to $PM_{2.5}$ samples collected in an urban-industrial area of Northern Italy. An innovative technique for the detachment and suspension in water of the whole intact dust from membrane filters was applied to expose the model organism to both the soluble and insoluble fractions of $PM_{2.5}$, which were analyzed for 34 elements by ICP-MS. Oxidative stress induced by PM on *A. thaliana* was assessed by light microscopic localization and UV–Vis spectrophotometric determination of superoxide anion ($\cdot O_2^-$) content on the exposed seedlings by using the nitro blue tetrazole (NBT) assay. The results showed a good efficiency and sensitivity of the method for PM mass concentrations >20 µg m^{-3} and an increase in $\cdot O_2^-$ content in all exposed seedlings, which mainly depends on the concentration, chemical composition, and sources of the PM administered to the model organism. Particles released by biomass burning appeared to contribute more to the overall toxicity of PM. This method was found to be cost-effective and easy to apply to PM collected on membrane filters in intensive monitoring campaigns in order to obtain valuable information on the ability of PM to generate oxidative stress in living organisms.

1. Introduction

The World Health Organization (WHO) estimated that exposure to air pollution causes 6.5 million deaths per year worldwide (WHO, 2016). Particulate matter is considered one of the most harmful air pollutants to human health and has been classified as a 'group 1 carcinogen' by the International Agency of Research on Cancer (Loomis et al., 2013).

In several studies, PM mass concentration has been used as an exposure indicator to assess the relationships between exposure to different concentrations of particulate matter (PM) with aerodynamic diameters of <10 µm (PM_{10}), 2.5 µm ($PM_{2.5}$) and 1 µm (PM_1) and adverse effects on human health (Williams et al., 2003; Zhang and Li, 2015; Lavigne et al., 2021). However, this metric only gives partial information about the ability of PM to generate adverse health effects and it does not consider the chemical composition of PM itself (Mirowsky et al., 2015; Ramírez et al., 2020).

The chemical and physical characteristics of PM have been extensively studied and recognized as primary metrics for assessing its adverse effects. However, there is still a gap in knowledge on the link between the concentration and composition of PM and its overall toxicity, and there is no clear definition of the multiple mechanisms behind it. Over the last years, oxidative stress has been recognized as one of the main mechanisms by which PM generates adverse health effects (Costantini, 2019; Øvrevik, 2019). Oxidative potential, which is a descriptor of the ability of particles to generate reactive oxygen species (ROS), has been proposed as a valuable indicator for estimating the toxicological potential of PM (Crobeddu et al., 2017; Molina et al., 2020). Chemical oxidative potential (OP) acellular assays have experienced increasing popularity as they are cheap, rapid, and user-friendly, and can be thus easily applied to several PM samples from air quality monitoring campaigns (Bates et al., 2019; Daellenbach et al., 2020). However, these assays show different sensitivity in relation to the chemical characteristics and sources of PM (Øvrevik, 2019; Massimi

et al., 2020b), their response depends on the operating conditions (e.g., reagent concentration, sample storage; Frezzini et al., 2022a,b), and the relationships between OP values and the toxicological potential of PM are still not entirely clear (Lionetto et al., 2021).

More complex systems for the assessment of PM toxicity involve the use of cell lines (e.g., lung epithelial cells, hepatoma cells, monocyte-macrophage cells) or model/experimental organisms (e.g., *Arabidopsis thaliana* seedling, *Caenorhabditis elegans* nematode, *Danio rerio* zebrafish, and *Drosophila melanogaster* midge) (de Santana et al., 2018; Piacentini et al., 2019; Ficociello et al., 2020; Manjunatha et al., 2021).

In commonly used cellular assays, cell lines are exposed in-vitro to PM extracts, and multiple endpoints (e.g., cell viability, DNA damage, activation of enzymatic responses, intracellular ROS production) are evaluated (Romani et al., 2018; Marchetti et al., 2019; Martin et al., 2019). However, these tests are usually quite expensive and require relatively long application times, making it difficult to apply them to many PM samples. In addition, some recent studies report a technique, i. e., the Air Liquid Interface cell culture (ALI), which allows the exposure of lung epithelial cells to the atmosphere in real-world conditions (Gualtieri et al., 2018; Costabile et al., 2019). Although these methods have proven good performance in determining the cellular oxidative response to PM, the information provided is only partial since it involves simple isolated cells that cannot reflect the complexity of an entire living organism.

The use of model/experimental organisms can be more efficient for a thorough understanding of how PM generates oxidative damage and cytotoxic outcomes inside complete organisms (Peixoto et al., 2017). Duan et al. (2017) and Manjunatha et al. (2021) recognized *D. rerio* as a suitable model animal organism to study PM-induced toxic effects. Other studies demonstrated that *C. elegans* can be an excellent candidate to assess the adverse effects of PM, especially for long-term exposure (de Santana et al., 2018; Chung et al., 2019; Ficociello et al., 2020). On the other hand, Piacentini et al. (2019) showed that exposure of the plant model organism *A. thaliana* to selected PM-components with different chemical-physical properties can induce oxidative stress and significantly alter the development of the root system, proposing this plant as a valid model organism for further studies on PM toxicity. Indeed, *A. thaliana* has some characteristics such as a completely sequenced genome, rapid growth, short life cycle, and easy availability, making it a widely used model organism. However, the use of model organisms still suffers from some critical issues related to high costs and long application times that make their use difficult in air quality monitoring campaigns in which large numbers of PM samples are obtained.

This study aims to propose an innovative, simple, rapid, and cost-effective method, applicable to intensive PM monitoring campaigns, for the assessment of the potential of different PM samples to induce oxidative stress in living organisms. To this aim, *A. thaliana* seedlings were exposed to certified urban dust and to $PM_{2.5}$ samples collected in an urban-industrial area of Northern Italy. Oxidative stress was assessed by superoxide anion localization and spectrophotometric determination on the exposed seedlings, the sensitivity of the method was tested, and the relationships between oxidative stress generation and concentration, chemical composition, and sources of the PM samples were assessed.

2. Materials and methods

2.1. Sample collection

This study used two types of samples: urban dust certified for its elemental content (NIST1648a, National Institute of Standards and Technology, U.S. Department of Commerce Gaithersburg), and $PM_{2.5}$ samples. NIST1648a elemental content is reported by Marcoccia et al. (2017) and Simonetti et al. (2018) and its effects on the *A. thaliana* root system have already been tested by Piacentini et al. (2019).

60 $PM_{2.5}$ samples were collected on polytetrafluoroethylene (PTFE) membrane filters (Pall-Gelmann, diameter 47 mm, porosity 2 μm) at an urban-industrial monitoring site: Cassana (44°51′4″N; 11°32′56″E; Canepari et al., 2014, Perrino et al., 2014) using a sequential sampler SWAM Dual Channel (FAI Instruments, Fonte Nuova, RM, Italy) equipped with a sampling head system certified for $PM_{2.5}$ and working at the flow rate of 2.3 m^3 h^{-1} with a 24-h time resolution. The 60 $PM_{2.5}$ samples were collected during two different sampling periods from September 25th to October 24th, 2020 (n. 30 filed filters), and from 25th September 2021 to 24th October 2021 (n. 30 filed filters). Cassana monitoring site is in the province of Ferrara, in the Eastern Po Valley (Emilia-Romagna, Northern Italy). It has been chosen as a collection site because in this area there are several local PM emission sources (biomass burning, vehicular traffic, industrial emissions, and a waste incineration plant) and it is characterized by frequent extended periods of high atmospheric stability, especially during winter (Canepari et al., 2014), which enhance the accumulation of air pollutants and increase PM concentrations.

2.2. Sample preparation

The 60 $PM_{2.5}$ samples collected by the sequential sampler SWAM Dual Channel (FAI Instruments, Fonte Nuova, RM, Italy) working at the flow rate of 2.3 m^3 h^{-1} with a 24-h time resolution were subjected to an innovative technique (Massimi et al., 2022b) for the detachment and suspension in water of the whole intact dust from the PTFE membrane filters (Pall-Gelmann, diameter 47 mm, porosity 2 μm). This procedure was demonstrated to be efficient for the recovery of the elements and to keep the oxidative potential of the detached dust unaltered (Frezzini et al., 2022a,b). This innovative method has the advantage of considering in the evaluation of the toxicological potential of PM not only the soluble fraction but also the insoluble fraction, which is usually not considered in PM toxicology studies (Palleschi et al., 2018; Alves et al., 2020). The efficiency of this method for the PM_{10} recovery from PTFE membrane filters was evaluated by Massimi et al. (2022b) by comparing the elemental content obtained by brushing the filters to that measured by applying a conventional procedure on 20 pairs of equivalent PM_{10} filters. The high recovery percentage of elements, the very-high linear correlation coefficients, and the low relative percentage differences with respect to the conventional procedure for elemental analysis of PM_{10} confirmed the efficiency of the toothbrush method as a quantitative procedure for the detachment and suspension in water of soluble and insoluble PM_{10} from PTFE membrane filters. However, the recovery of other PM_{10} components (such as organic species) and possible changes in particle size by applying this method, have not yet been assessed. Further details about this procedure are reported in Massimi et al. (2022b) and in Frezzini et al. (2022a,b). Each of the former 30 $PM_{2.5}$ filters, collected from September 25th to October 24th, 2020, was placed in a 50 mm diameter sterile Petri dish containing 2 mL of deionized water. The detachment of intact $PM_{2.5}$ was obtained mechanically, brushing each filter for 2 min with an electrical toothbrush with a sensitive brush head (Braun, Germany, Oral-B Vitality Sensitive) in order to obtain a water suspension containing both soluble species and insoluble particles, as extensively detailed by Massimi et al. (2022b). Then, the 2 mL water suspensions obtained from each of the 10 filters collected during the first 10 sampling days (from September 25th to October 4th, 2020) were merged into a single 20 mL sample (named sample A), thus obtaining a final $PM_{2.5}$ water suspension representative of the first 10 sampling days. The same procedure was repeated for the 10 filters of the next 10 days (sample B, from October 4th to October 14th, 2020) and for the 10 filters of the last 10 days (sample C, from October 14th to October 24th, 2020) in order to obtain three water-suspensions (named A, B, and C, respectively), each representative of 10 consecutive sampling days, containing 0.07, 0.11 and 0.23 g L^{-1} of $PM_{2.5}$, respectively. Finally, 10 blank PTFE membrane filters were subjected to the same procedure (i.e. brushing each filter for 2 min with an electric toothbrush with a sensitive head in a 50 mm diameter sterile Petri dish containing 2 mL of deionized water and merging the obtained solutions into a single 20 mL sample) in

replicate to obtain two control samples (Control).

The other 30 PM$_{2.5}$ filters collected from 25th September 2021 to 24th October 2021 were subjected to the same toothbrush detachment procedure (Massimi et al., 2022b) but in a 50 mm diameter sterile Petri dish containing 5 mL of deionized water. The 30 obtained PM$_{2.5}$ water suspensions of 5 mL each were merged into a single 150 mL final sample. This stock solution was then diluted to obtain 5 duplicate samples containing 0.036, 0.064, 0.11, 0.14, and 0.18 g L^{-1} of PM$_{2.5}$, respectively. Again, two control samples were obtained by performing the same procedure on blank PTFE membrane filters.

2.3. Sample elemental analysis

Each PM$_{2.5}$ water suspension obtained was analyzed for 34 elements (Al, As, B, Ba, Bi, Ca, Cd, Ce, Co, Cr, Cs, Cu, Fe, Ga, K, La, Li, Mg, Mn, Mo, Na, Nb, Pb, Rb, Sb, Sn, Sr, Ti, Tl, U, V, W, Zn, Zr) by applying a procedure extensively described in Massimi et al. (2022b).

Briefly, the 10 mL water suspensions were subjected to mechanical agitation for 30 min and then filtered using cellulose nitrate filters (NC filters; pore size 0.45 μm, Merck Millipore Ltd., Billerica, MA, USA) to separate the soluble from the insoluble fraction of PM. Cellulose nitrate filters, containing the insoluble fraction, were subjected to acid digestion in a microwave oven for 52 min at 180 °C. For the acid digestion, 2 mL of ultrapure nitric acid (HNO$_3$) (65 %, RPE, Carlo Erba, Rome, Italy) and 1 mL of hydrogen peroxide (H$_2$O$_2$) (30 %, Suprapur, Merck) were used. Then the digested solution was diluted into 50 mL of deionized water and filtered through syringe cellulose nitrate filters (NC filters; pore size 0.45 μm, Merck Millipore Ltd., Billerica, MA, USA). Finally, the elements in the soluble and insoluble fraction were analyzed by inductively coupled plasma mass spectrometry (ICP-MS) with quadrupole mass detection, equipped with a glass nebulizer (0.4 mL min^{-1}; Analytik Jena AG, Jena, Germany). The external standard calibration curve for each element was performed by serially diluting standard stock solutions (1000 ± 2 mg L^{-1}; Exaxol Italia Chemical Manufacturers Srl, Genoa, Italy; Ultra Scientific, North Kingstown, RI, USA; Merck Millipore Ltd., Billerica, MA, USA) in the range 1–500 μg L^{-1}. Yttrium (1000 ± 2 mg L^{-1}; Panreac Qumica, Barcelona, Spain) was used as an internal standard for all measurements to control nebulizer efficiency. The instrumental conditions and performance of the method were according to Canepari et al. (2009).

The limit of detection (LOD) of each variable was set as mean plus 3 times the standard deviation (SD) of 10 replicate blank determinations (supplementary materials; Table S1.2). The total element concentration was calculated as the sum of the soluble and insoluble fractions (the concentrations of all the analyzed soluble and insoluble elements for each PM$_{2.5}$ water suspension administered to *A. thaliana* seedlings are reported in supplementary materials S.3 and S.4).

2.4. A. thaliana exposure

Seeds of Col-0 ecotype of *Arabidopsis thaliana* (L.) Heynh were surface sterilized with 70 % ethanol (C$_2$H$_5$OH; Carlo Erba, Rome, Italy) plus 0.1 % sodium dodecyl sulfate (SDS; Sigma-Aldrich, Milan, Italy) solution for 5 min, and then soaked and mechanically shaken at 250 rpm in a solution of 20 % sodium hypochlorite (NaClO; Carlo Erba, Rome, Italy) plus 0.1 % SDS for 25 min. To remove traces of sodium hypochlorite, the seeds were subsequently washed four times with sterile deionized water. Then, the seeds were sown on a medium containing half-strength (2.1 g L^{-1}) Murashige and Skoog Basal Medium (Duchefa Biochemie BV, Haarlem, The Netherlands) (Classic Murashige and Skoog, 1962), 0.7 % sucrose, and 0.7 % agar, at pH 5.8. The media were supplemented or not (Control) with different concentrations (i.e., 0.5, 1, 2, and 5 g L^{-1}) of urban dust certified for its elemental content, with the PM$_{2.5}$ samples A, B, and C described above, and with the water suspensions containing increasing concentrations of PM$_{2.5}$ mass (i.e., 0.036, 0.064, 0.11, 0.14, and 0.18 g L^{-1}) with the same chemical composition.

Seeds were grown in round Petri dishes for 14 days at 21 ± 2 °C during the night and 23 ± 2 °C during the day, 70 % relative humidity, photoperiod of 16 h of light and 8 h of dark per day and at 210 μmol m^2 s^{-1} intensity of white light. Seedlings exposed to the certified urban dust and to the A, B, and C PM$_{2.5}$ samples were separately grown in large Petri dishes (n = 24 seeds per dish), while the seedlings exposed to the water suspensions with increasing concentrations of PM$_{2.5}$ mass were grown in small Petri dishes (n = 8 seeds per dish), which allowed the tests to be applied on seedlings grown in a smaller culture medium volume and therefore with a greater concentration of suspended PM$_{2.5}$ mass.

2.5. Localization and analysis of superoxide anion content in A. thaliana seedlings

Oxidative stress was evaluated by intracellular localization and determination of superoxide anion (•O$_2^-$) production after exposure of *A. thaliana* seedlings to the different samples by using the Nitro blue tetrazole (NBT; Roche Diagnostics Corp., Gmbh, Germany) assay. This assay is based on the highly specific reaction that occurs between NBT and •O$_2^-$, the main product of which is a purple/blue precipitate named formazan that is clearly visible by observation under a light microscope and that can be quantified by UV–Vis spectrophotometric analysis.

For •O$_2^-$ visualization, the roots of *A. thaliana* (5 seedlings per treatment) were immersed into a solution containing 0.5 mg L^{-1} of NBT in 10 mM Tris-HCl buffer (pH 7.40 ± 0.05; Sigma-Aldrich, Milan, Italy) and incubated in the dark at room temperature (RT) for 30 min. Then, the roots were rinsed with the buffer solution to stop the reaction, immersed in a chloral hydrate solution ((Cl$_3$CCH(OH)$_2$); Sigma-Aldrich, Milan, Italy) and incubated in the dark for 24 h at 8 °C. Finally, the roots were observed by using a LEICA DMRB light microscope (Leica Microsystems, Wetzlar, Germany), equipped with Nomarsky optics.

For •O$_2^-$ determination, the procedure suggested by Demecsová et al. (2020) was followed: ~200 mg (fresh weight) of seedlings were weighed after exposure through an analytical balance (Kern ABT 220-5DNM; Kern & Sohn, Balingen, Germany) and incubated in the dark at RT for 1 h in a solution containing 0.5 mM NBT and 10 mM sodium azide (NaN$_3$; Sigma-Aldrich, Milan, Italy) in 20 mM sodium phosphate buffer (pH 6.0). Then, the seedlings were rinsed with deionized water and homogenized with a mortar and pestle by adding liquid nitrogen. The homogenates were suspended by adding 180 μL of 2 M potassium hydroxide (KOH; Sigma-Aldrich, Milan, Italy) solution, 220 μL of dimethyl sulfoxide (DMSO; Duchefa Biochem, Haarlem, the Netherlands), and 200 μL of 2-propanol (Carlo Erba, Rome, Italy) and then incubated for 1 h in the dark at RT. Then, the homogenates were centrifuged (Micro Star 17 centrifuge, VWR, Milan, Italy) for 5 min at 10,000 rpm. After centrifugation, the supernatant was taken and the •O$_2^-$ content was analyzed by measuring the formazan absorbance at the 630 nm wavelength by UV–Vis spectrophotometry (Varian Cary 50 Bio UV–Vis; Varian Inc., Palo Alto, CA, USA). The absorbance signal recorded for each treatment was multiplied by the dilution factor of the extracted solution and normalized by the weight of each *A. thaliana* sample (absorbance g^{-1}).

Each treatment was performed in duplicate. The percentage standard deviation for the two replicates of each treatment is <20 %, demonstrating the good repeatability of the experiments. The paired-sample *t*-test was used to observe the significance of the differences in the values obtained for each treatment compared to Control. A p-value of <0.05 was considered statistically significant.

2.6. Additional analyses on A. thaliana seedlings exposed to certified urban dust

Given the large availability of certified urban dust, which does not require specific samplings for its collection like PM$_{2.5}$ samples, additional analyses were carried out on *A. thaliana* seedlings exposed to

increasing concentrations of certified urban dust to obtain useful information about the interaction of *A. thaliana* with elements in PM and about the overall stress state of the plant model organism after exposure to PM. In particular, elements' bioaccumulation and total chlorophyll content were assessed on the *A. thaliana* seedlings exposed or not (Control) to different concentrations (0.5, 1, 2, and 5 g L^{-1}) of certified urban dust.

For the elements' bioaccumulation analyses, 0.1 g (dry weight) of the seedlings and 0.1 g of the culture medium for each treatment were acid digested and analyzed for 34 elements (Al, As, B, Ba, Bi, Ca, Cd, Ce, Co, Cr, Cs, Cu, Fe, Ga, K, La, Li, Mg, Mn, Mo, Na, Nb, Pb, Rb, Sb, Sn, Sr, Ti, Tl, U, V, W, Zn, Zr) by ICP-MS. The seedlings were weighed (analytical balance Kern ABT 220-5DNM; Kern & Sohn, Balingen, Germany) after being oven-dried (WTC binder FD53 drying oven; BINDER GmbH, Tuttlingen, Germany) at a temperature of 60 °C for 72 h. Then, the seedlings and the culture medium of each treatment were subjected to acid digestion in a microwave oven for 52 min at 180 °C, using 2 mL of ultrapure nitric acid (HNO$_3$) (65 %, RPE, Carlo Erba, Rome, Italy) and 1 mL of hydrogen peroxide (H$_2$O$_2$) (30 %, Suprapur, Merck). Each digested solution was then diluted to 50 mL of deionized water and filtered through syringe cellulose nitrate filters (NC filter; pore size 0.45 μm, Merck Millipore Ltd., Billerica, MA, USA). Finally, the 34 elements were analyzed by ICP-MS using the same procedure and instrumental conditions reported in paragraph 2.3. The bioaccumulation factor was calculated by the ratio of the concentration of elements within seedling tissues to the concentration of elements in the culture media at the end of the growth period.

For the assessment of total chlorophyll content, 0.1 g (fresh weight) of leaves from seedlings of each treatment were taken and homogenized using a mortar and a pestle with the addition of liquid nitrogen. Then, the homogenates were suspended in 1 mL of *N, N*-dimethylformamide

(DMF; Sigma-Aldrich, Milan, Italy) and centrifuged (Micro Star 17 centrifuge, VWR, Milan, Italy) for 10 min at 10,000 rpm. Finally, the supernatants were collected and the absorbances (A) at the 664 nm and 647 nm wavelengths were measured by UV–Vis spectrophotometry (Varian Cary 50 Bio UV–Vis; Varian Inc., Palo Alto, CA, USA) to record the absorbance signal of the chlorophyll *a* and b, respectively. The total chlorophyll content was obtained by applying the following equation (Inskeep and Bloom, 1985):

$$\left[\text{Total chlorophyll content } \left(\text{mg L}^{-1} \right) \right] = 17.90 * A647 + 8.08 * A664$$

The value obtained for each treatment was multiplied by the dilution factor of the extracted solution and normalized by the weight of each *A. thaliana* sample (mg Kg^{-1}).

Also in this case, each treatment was performed in duplicate. The percentage SD for the two replicates of each treatment is <30 %. The paired-sample *t*-test was used to observe the significance of the differences in the values obtained for each treatment compared to Control. A p-value of <0.05 was considered statistically significant.

3. Results and discussion

3.1. Superoxide anion assessment in A. thaliana seedlings exposed to certified urban dust

To assess *A. thaliana* oxidative stress induced by exposure to increasing concentrations of certified urban dust, the content of superoxide anion in the extracts of the exposed *A. thaliana* seedlings was evaluated. As can be seen from Fig. 1, from an initial macroscopic morphological analysis, the seedlings of *A. thaliana* appear to grow less and lose color as the concentration of certified urban dust increases, thus
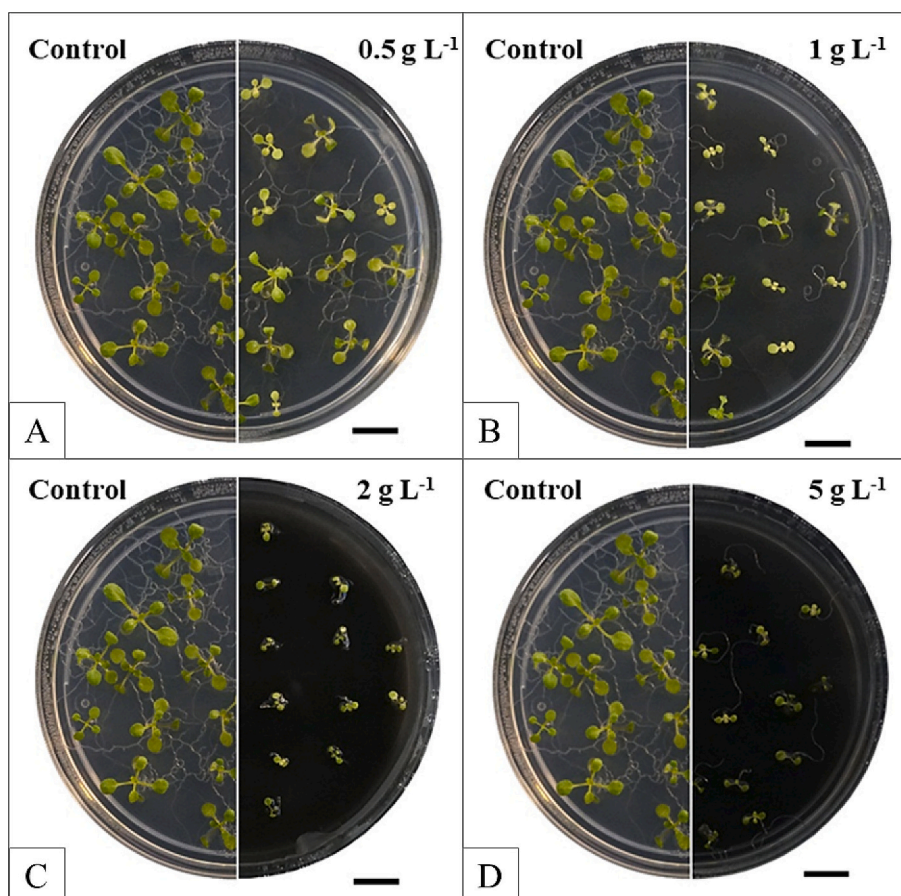

Fig. 1. *A. thaliana* seedlings grown for 14 days in the presence of 0.5 g L^{-1} (A), 1 g L^{-1} (B), 2 g L^{-1} (C), and 5 g L^{-1} (D) of certified urban dust. Bars: 1 cm.

showing a reduction in growth and health status when exposed to 0.5, 1, 2 and 5 g L^{-1} of urban dust.

The results obtained from superoxide anion determination by UV–Vis spectrophotometry show an increase in the absorbance signal of formazan, and thus an increase of $^{\bullet}O_2^-$ as the concentration of urban dust increases (Fig. 2). In particular, at the concentrations of 0.5, 1, and 2 g L^{-1}, the signal respectively increased by 18 %, 28 %, and 64 % compared to Control, while at the concentration of 5 g L^{-1} the strongest signal was recorded, with an increase of 86 % compared to Control (the mean formazan absorbance signal values are reported in supplementary materials; Table S1.1).

These results reveal that one of the major mechanisms by which PM exerts its toxicity in *A. thaliana* is related to the triggering of oxidative stress and confirm the effectiveness of this method for the assessment of ROS production in the plant model organism. Moreover, to study changes in the intracellular localization of superoxide anion in response to the different PM concentrations, formazan was visualized by light microscope in the root system (i.e., primary and secondary roots) of *A. thaliana* seedlings because, in our experimental conditions, it is the first plant organ to be exposed to the pollutants and consequently from which an alteration of the redox status could arise (Fig. 3).

In Control conditions, the NBT-staining was weak and confined both in the elongation zone and in the differentiated region of the primary root, as well as at the basal part of the lateral root, as expected (Fig. 3, A–C). Under 0.5 g L^{-1} of urban dust, the signal was stronger with respect to Control and mainly localized in the elongation zone and in the vasculature of the mature part of the primary roots, while in the lateral roots, it was localized at the base zone like the Control (Fig. 3, D–F). The NBT signal in the primary roots exposed to 1 g L^{-1} was like that of 0.5 g L^{-1} except for a wider localization in the root cap (Fig. 3 G, arrow) and in the root meristem, and in the cortical cells of the elongation zone.

In the lateral root, the signal appeared evident also in the elongation zone and occasionally in the meristem (Fig. 3, G–I). At the concentration of 2 g L^{-1}, the NBT signal was more diffuse, covering almost every part of both primary and lateral roots. In particular, the staining was evident in the vasculature of the primary root and especially in the root meristem of both primary and lateral roots, which is a root zone where oxidative species are usually produced at very low levels (Fig. 3, J–L, arrows) (Zhou et al., 2020). Root meristem contains pluripotent stem cells, which are maintained during the whole lifespan of the plant and from which the post-embryonic development of the entire root depends. It has been shown that during physiological conditions, low and tightly regulated levels of ROS are needed for the root stem cells' maintenance by acting on specific proteins, transcription factors, and hormone levels (Zwiewka et al., 2019). On the contrary, an increase in ROS content and spread inside the root meristem is often reported during abiotic stress conditions, leading to the inhibition of root development (Zwiewka et al., 2019). Thus, the presence of a strong NBT staining in the meristem of both primary and lateral roots induced by the urban dust exposures indicates an intracellular redox imbalance which can lead to root morphological/developmental alterations, as previously reported in Piacentini et al., 2019. Finally, the formazan signal in the roots exposed to the highest concentration (5 g L^{-1}) of urban dust showed the strongest and the wider intensity of the signal, especially in the distal cells of the root meristem and in the stele of the elongated region (Fig. 3, M–O). Interestingly, the lateral roots of *A. thaliana* seedlings grown in the presence of the highest urban dust concentration show a strong histochemical signal even at the early stages of their development (Fig. 3, O).

The results highlighted that both intracellular production and localization of $^{\bullet}O_2^-$ in the different parts of the primary and secondary roots are strictly related to the concentration of the urban dust supplied in the culture medium. In particular, the staining intensity in the roots gradually increased together with the increasing concentration of the dust, becoming also more evident in those root tissue/zones where the oxidative species are usually kept at low levels, such as in the root apical meristem (Piacentini et al., 2021).

In this regard, the high ROS levels detected in the root meristem could be due to the presence of heavy metals inside this root zone which is known to be an accumulation area for these elements. Indeed, urban dust is rich in metals and metalloids such as As, Cd, Pb, and Ni, which are toxic even at low concentrations and able to generate oxidative stress through $^{\bullet}O_2^-$ production (Abozeid et al., 2017). In addition, the localization of superoxide anion at the level of the root meristem (and thus in newly formed tissues) after exposure to 2 g L^{-1} and 5 g L^{-1} highlights the presence of an early effect in seedlings exposed to urban dust. Collectively, despite the different origins (i.e., embryonic the former, post-embryonic the latter), the effects of PM on $^{\bullet}O_2^-$ localization/production in the primary and secondary roots were similar.
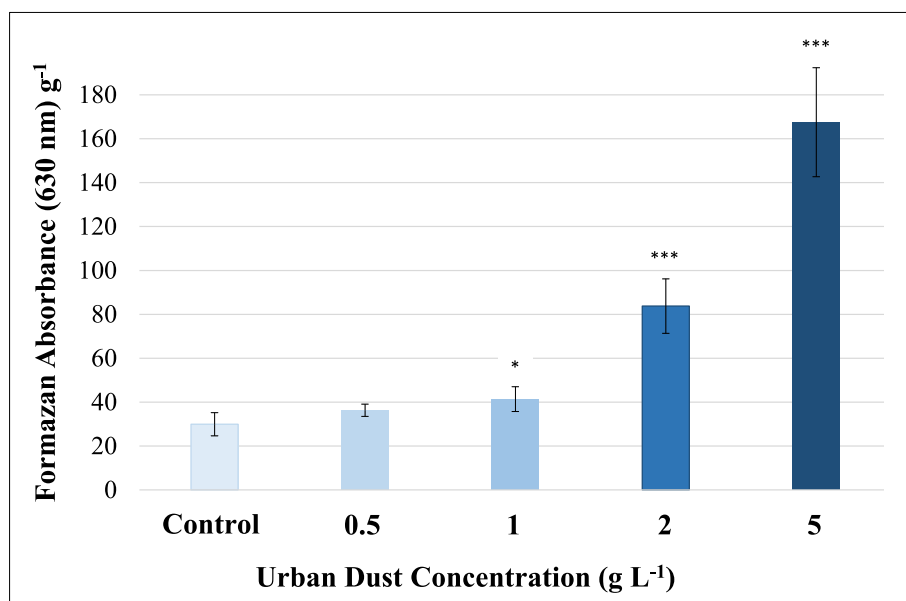

Fig. 2. Mean values ($\pm$SD) of formazan absorbance signal in the *A. thaliana* seedlings grown for 14 days in the presence of different urban dust concentrations (0.5, 1, 2, and 5 g L^{-1}); p-values of the paired-sample *t*-test between each treatment and Control: *** = p < 0.001; ** = p < 0.01; * = p < 0.05.
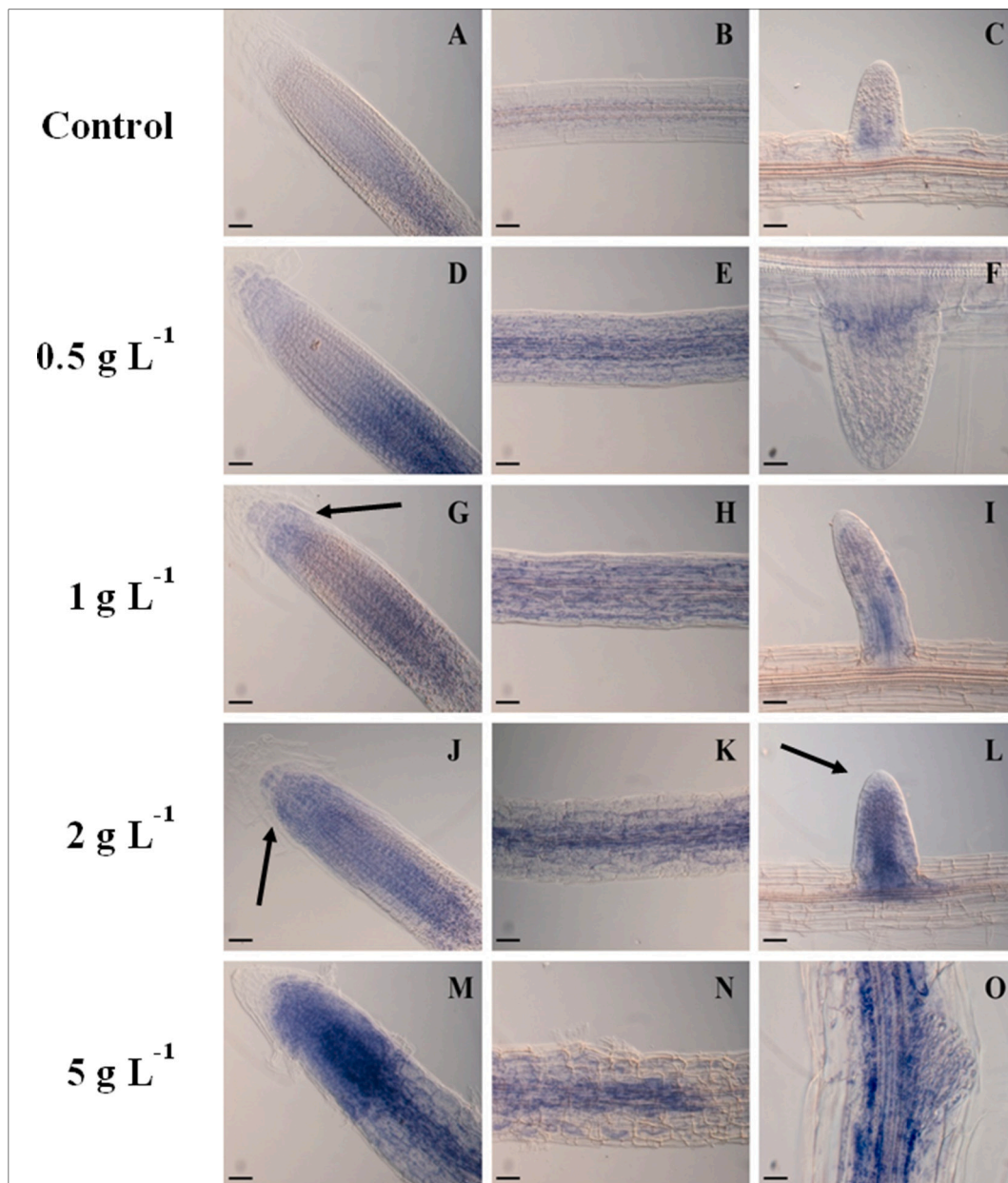
Fig. 3. Localization of superoxide anion ($^{\bullet}O_2^-$) detected by NBT staining in the primary and secondary roots of *A. thaliana* seedlings grown for 14 days in the presence of different urban dust concentrations. In detail: Control (A–C), 0.5 g L^{-1} (D–F), 1 g L^{-1} (G–I), 2 g L^{-1} (J–L), 5 g L^{-1} (M–O). Bars = 20 μm (F, O), 40 μm (A–E; G–N). N = 5 per treatment.

3.2. Assessment of elements' bioaccumulation and total chlorophyll content in A. thaliana seedlings exposed to certified urban dust

Fig. 4 shows the concentration of some elements of the certified urban dust in the culture media and in the exposed seedlings (elements accumulated by *A. thaliana*) after the growth period (LODs and concentrations of all the analyzed elements are reported in supplementary materials; Table S1.2). Toxic elements such as As and Cd (Farooq et al., 2016; Haider et al., 2021) are strongly accumulated in *A. thaliana*, while other less toxic elements such as La and Sn, are poorly bioaccumulated (Fig. 4). Other elements strongly accumulated in *A. thaliana* are Pb, Al, V, Fe, Co, Ni, Cu, and Cr (supplementary materials; Table S1.2).

These results confirm the selectivity of *A. thaliana* in the elements' accumulation and its capacity to hyper-accumulate As and Cd (Guo et al., 2008; Fattorini et al., 2017). The high concentration of these elements in the root system of *A. thaliana* seedlings may be the main cause

of stress due to exposure to urban dust (Cho and Seo, 2005; Piacentini et al., 2020).

To evaluate whether PM exposure leads to an overall stress effect proportional to the dust concentration to which the plant model organism is exposed, the total chlorophyll content in the areal portion of *A. thaliana* seedlings was assessed after exposure to the increasing concentrations of certified urban dust.

The results show a decrease in total chlorophyll content as the concentration of urban dust increases (Fig. 5). Specifically, at the highest concentration (5 g L^{-1}), a 71 % decrease in chlorophyll content was observed compared to Control, while at the concentrations of 0.5, 1, and 2 g L^{-1} a decrease of 32 %, 50 %, and 58 % was recorded, respectively (Fig. 5).

These findings reveal that the stress induction on *A. thaliana* photosynthetic organs is strongly correlated and proportional to urban dust concentration in the culture medium (mean values of total
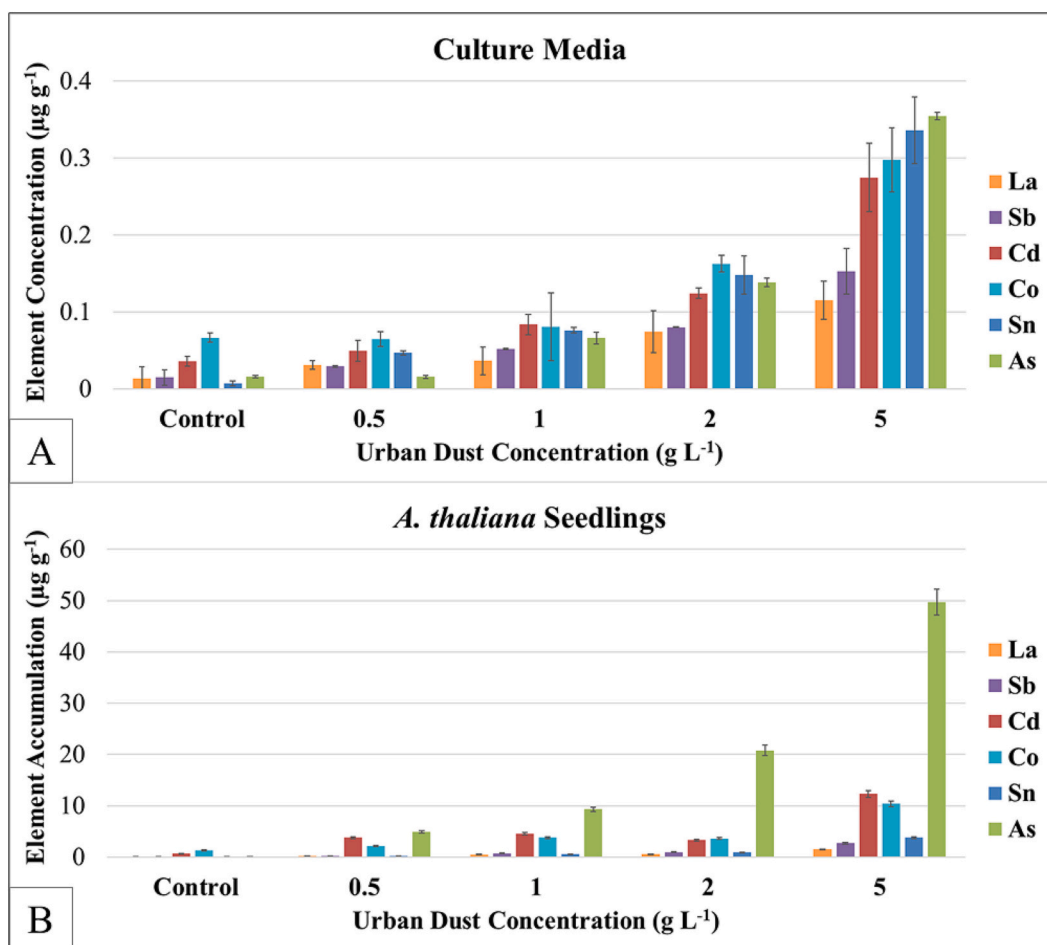
Fig. 4. Mean concentrations (±SD) of elements in the culture media (A) and in *A. thaliana* seedlings (B) at the end of the cultural period in the presence of different urban dust concentrations.

chlorophyll content are reported in supplementary materials; Table S1.4). Based on these results, it can be confirmed that urban PM generates important stress phenomena in *A. thaliana* seedlings, confirming the suitability of this plant as a model organism in PM toxicology studies.

3.3. Superoxide anion assessment in A. thaliana seedlings exposed to PM$_{2.5}$ samples

To assess the possible use of *A thaliana* as a model organism to study the oxidative stress effects induced by PM collected on membrane filters and, therefore, to evaluate the suitability of this method in air quality monitoring campaigns, the NBT assay, previously applied to the certified urban dust, was applied to the PM$_{2.5}$ samples collected in the PM monitoring campaign carried out at Cassana site. Superoxide anion production was assessed on the *A. thaliana* seedlings exposed to the samples A, B, and C, each representative of 10 consecutive sampling days (from September 25th to October 24th, 2020) and containing 0.07, 0.11, and 0.23 g L^{-1} of PM$_{2.5}$, respectively.

From Fig. 6, we can observe that PM$_{2.5}$ mass concentration is very different in the three sampling periods A, B, and C. In fact, during the first 10 sampling days (A, mean PM$_{2.5}$ mass concentration = 10.5 µg m^{-3}) the study area was characterized by low PM$_{2.5}$ mass concentration due to lower atmospheric stability and greater dilution of air masses. However, during this period, a small event of Saharan dust incursion occurred as confirmed by back-trajectory models (NOAA HYSPLIT MODEL, backward trajectory ending at 0900 UTC 03 Oct 20; GDAS Meteorological Data; supplementary materials; Fig. S2.1).

Instead, the second 10 days (B, mean PM$_{2.5}$ mass concentration = 17 µg m^{-3}) are characterized by a short period of atmospheric stability which led to an increase of PM$_{2.5}$ mass concentrations. Finally, the last 10 days (C, mean PM$_{2.5}$ mass concentration = 34 µg m^{-3}) were characterized by a strong atmospheric stability period that enhanced PM$_{2.5}$ mass concentrations (the trends of the atmospheric stability periods are confirmed by natural radioactivity measurements, whose results are reported in supplementary materials; Fig. S2.2).

The results from the elemental analyses, instead, show that sample A is mainly characterized by the presence of the insoluble fraction of Cs, K, Rb, Al, Mg, Ce, and La, usually associated with crustal dust and mainly derived from natural emission sources (supplementary materials; Table S3.1) (Canepari et al., 2019; Massimi et al., 2022a; Pant and Harrison, 2013). The presence of relativity high concentrations of soil dust tracers can be related to the small Saharan dust incursion event that occurred during the first 10 sampling days. On the other hand, samples B and C show high concentrations of the soluble fraction of Cs, K, Rb, and Li that can effectively trace PM from biomass burning emissions (Saggu and Mittal, 2020; Massimi et al., 2020a; Perrino et al., 2010) as well as high concentrations of soluble V and Ti, which are commonly associated to PM from heavy oil combustion (supplementary materials; Table S3.1) (Belis et al., 2015). In addition, in both these samples, high concentrations of soluble Bi, Cd, Mo, Mn, Sb, Sn, Pb, Zn, and W, typically associated with industrial emission sources of PM (Mooibroek et al., 2022), were found. Moreover, samples B and C show high concentrations of insoluble Sb and Sn, mainly associated with non-exhaust traffic emissions of PM from mechanical abrasion of vehicle brakes (Celo et al., 2021) (supplementary materials; Table S3.1).
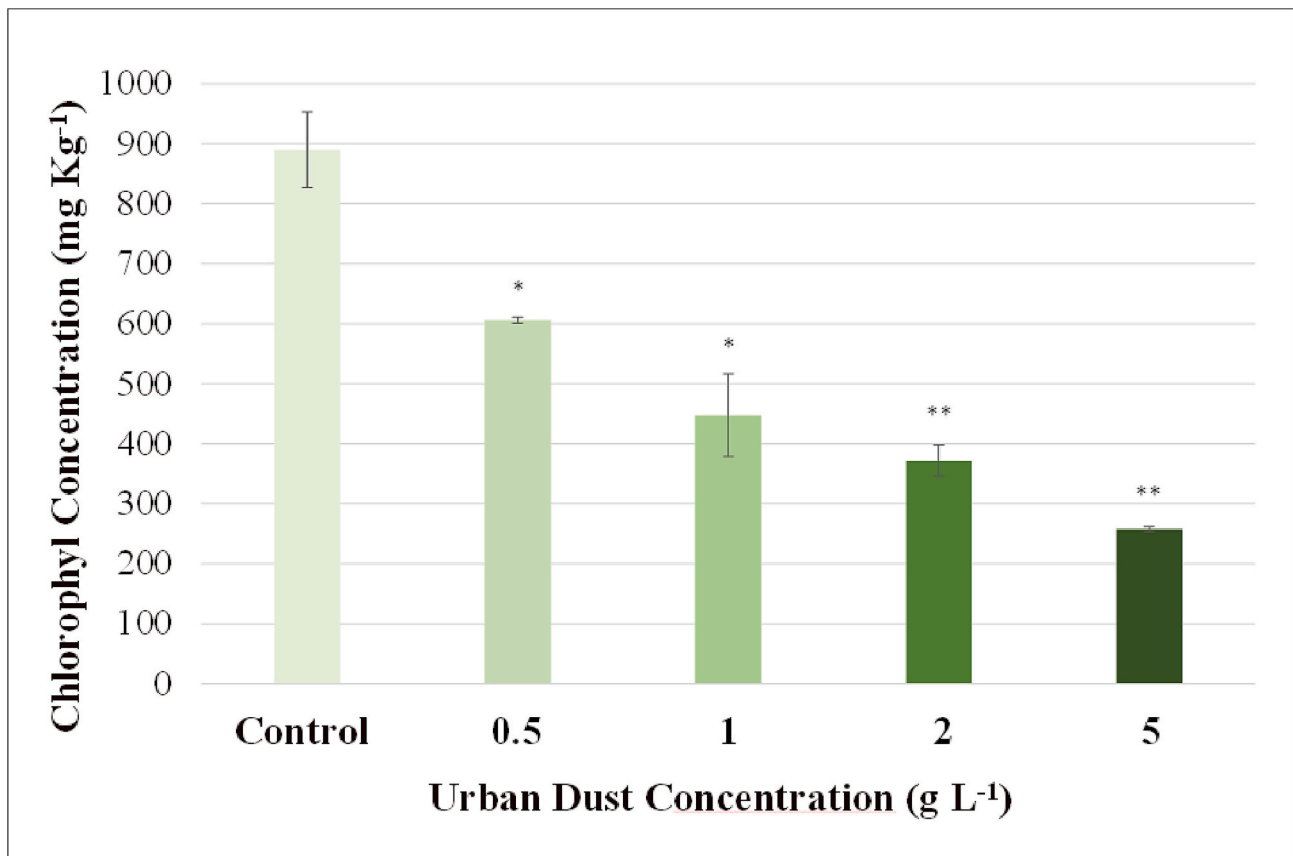
Fig. 5. Mean values (±SD) of total chlorophyll content in *A. thaliana* seedlings grown for 14 days in the presence of different urban dust concentrations (0.5, 1, 2, and 5 g L^{-1}); p-values of the paired-sample *t*-test between each treatment and Control: *** = p < 0.001; ** = p < 0.01; * = p < 0.05.

In this case, the different PM$_{2.5}$ samples do not appear to affect macroscopically the morphology and the state of growth and health of the *A. thaliana* seedlings (supplementary materials; Fig. S3.1). However, as can be seen from Fig. 7, statistically significant differences compared to Control were found in the superoxide anion content. The formazan absorbance signal in the seedling exposed to sample A does not show significant differences compared to Control, while in the seedlings exposed to samples B and C, the formazan signal is significantly higher with respect to Control (Fig. 7). In particular, the seedlings exposed to sample B show a 29 % increase in absorbance signal compared to Control, while the seedlings exposed to sample C show an increase of 66 %. The results obtained from this analysis are consistent with the different mass concentrations and chemical composition and sources of the PM$_{2.5}$ to which the seedlings were exposed. In fact, the generation of $^\bullet O_2^-$ and thus of oxidative stress was greater in the *A. thaliana* seedlings exposed to sample B and even more so in the seedlings exposed to sample C, in which the highest PM$_{2.5}$ mass and toxic element (such as Cd, Sb, Pb, and Zn) concentrations were present. Furthermore, in sample C the concentration of the soluble fraction of elements such as Cs, K, Rb, and Li, which are tracers of PM from biomass burning emissions (Massimi et al., 2020a), was considerably higher than in samples A and B. Thus, it is reasonable to hypothesize that particles released from this emission source contribute more to the overall toxicity of PM. This evidence is in agreement with previous findings on PM stress effects on *A. thaliana* exposed to atmospheric dust with different chemical-physical properties (Piacentini et al., 2019). On the contrary, the lower PM$_{2.5}$ mass and toxic element concentrations in sample A probably did not produce an amount of superoxide anion detectable by UV–Vis spectrophotometric analysis and thus, no statistically significant difference in oxidative stress was found for this treatment with respect to Control (mean formazan absorbance signal values are reported in supplementary

materials; Table S3.2). However, as shown by Fig. 8, which reports the observation by light microscope of the root system of the seedlings exposed to PM$_{2.5}$, a greater superoxide anion production after the exposure to sample A compared to Control was visible. In Control, the NBT-staining was weak and restricted to those root tissues involved in the cell elongation/differentiation processes, i.e., in the pro-vascular tissues of the primary root elongation zone and at the base of the secondary root primordia (Fig. 8 A and B, respectively) as well as in the vasculature of the root (Fig. 8 C). Compared to Control, the exposure to sample A increased the intensity and diffusion of the staining, especially in the meristematic zone of both primary and lateral roots (Fig. 8, D–E). In addition, the lateral roots treated with sample A showed the NBT signal starting up from the first phases of their organization (Fig. 8 F). Moreover, the roots exposed to samples B and C showed a strong signal in all the primary root tissues as well as in the lateral root primordia of lateral roots (Fig. 8, G–L). The high toxicity of the sample C is also evident by the cyto-histological damages (cellular hypertrophy, altered pattern of cell division/differentiation) observed, in particular, in the lateral roots of *A. thaliana* grown in the presence of this sample (Fig. 8 L, inset).

Overall, the greatest oxidative stress was recorded in the roots of the seedlings exposed to samples B and C and may be associated with the greater concentration of PM$_{2.5}$ mass and toxic elements in these samples.

The quantification of formazan absorbance signal by UV–Vis spectrophotometry coupled with localization of formazan by optical microscopy is therefore particularly effective for assessing PM-induced oxidative stress. However, the sensitivity of this method for application to single PM filters has to be evaluated, since the results here obtained concern the application of the proposed method on 10 daily PM$_{2.5}$ filters (collected at the flow rate of 2.3 m^3 h^{-1} with a 24-h time resolution) and thus do not allow to assess the suitability of the method for the
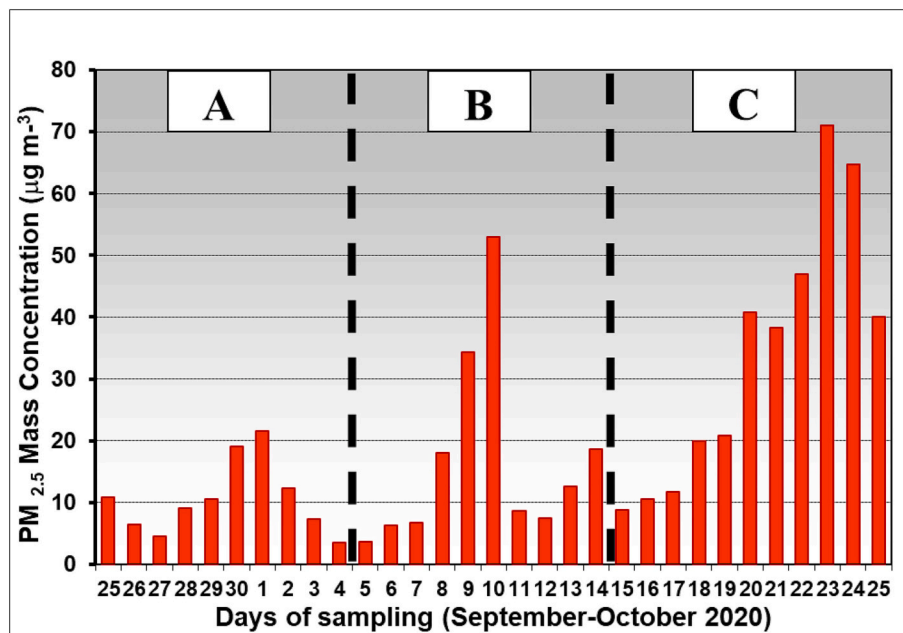
Fig. 6. Mass concentrations of $PM_{2.5}$ at Cassana site from September 25th to October 24th, 2020.
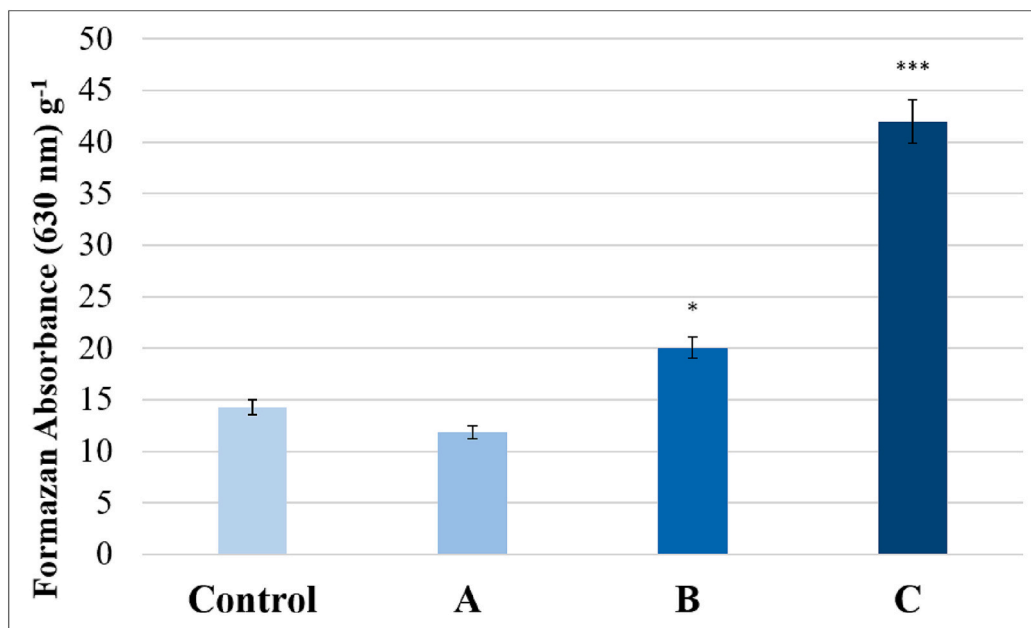

Fig. 7. Mean values ($\pm$SD) of formazan absorbance signal in *A. thaliana* exposed to A, B and C $PM_{2.5}$ samples; p-values of the paired-sample *t*-test between each treatment and Control: *** = $p < 0.001$; ** = $p < 0.01$; * = $p < 0.05$.

evaluation of oxidative stress generation by PM collected over a shorter time span.

3.4. Assessment of the sensitivity of the method

To test the sensitivity of the method, *A. thaliana* seedlings were exposed to 0.036, 0.064, 0.11, 0.14, and 0.18 g L^{-1} of $PM_{2.5}$; in the measurement period, in which the mean $PM_{2.5}$ mass concentration was 23 μg m^{-3}, this corresponds to 0.5, 0.9, 1.6, 2, and 2.5 daily $PM_{2.5}$ filters.

The elemental composition of the samples was similar to that obtained for samples B and C from the $PM_{2.5}$ filters collected from 25th September 2020 to 24th October 2020 (element concentrations of the $PM_{2.5}$ water suspension obtained from the 30 filters collected at Cassana

site from 25th September 2021 to 24th October 2021 are reported in supplementary materials; Table S4.1). A statistically significant response ($p < 0.01$) was obtained only for the seedlings exposed to 0.11, 0.14, and 0.18 g L^{-1} of $PM_{2.5}$, in particular, these treatments show an increase in the formazan absorbance signal of 52 %, 55 %, and 56 % compared to Control, respectively (Fig. 9) (mean formazan absorbance signal values are reported in supplementary materials; Table S4.2).

Overall, the proposed method could be effectively used to assess PM-induced oxidative stress on single 24-h filters with relatively high PM mass concentrations (>20 μg m^{-3}), while under conditions of lower air pollution and medium-low mass concentrations, it is necessary to merge 2–3 24-h PM filters to obtain quantitatively significant results. However, since through the use of light microscopy it is possible to detect
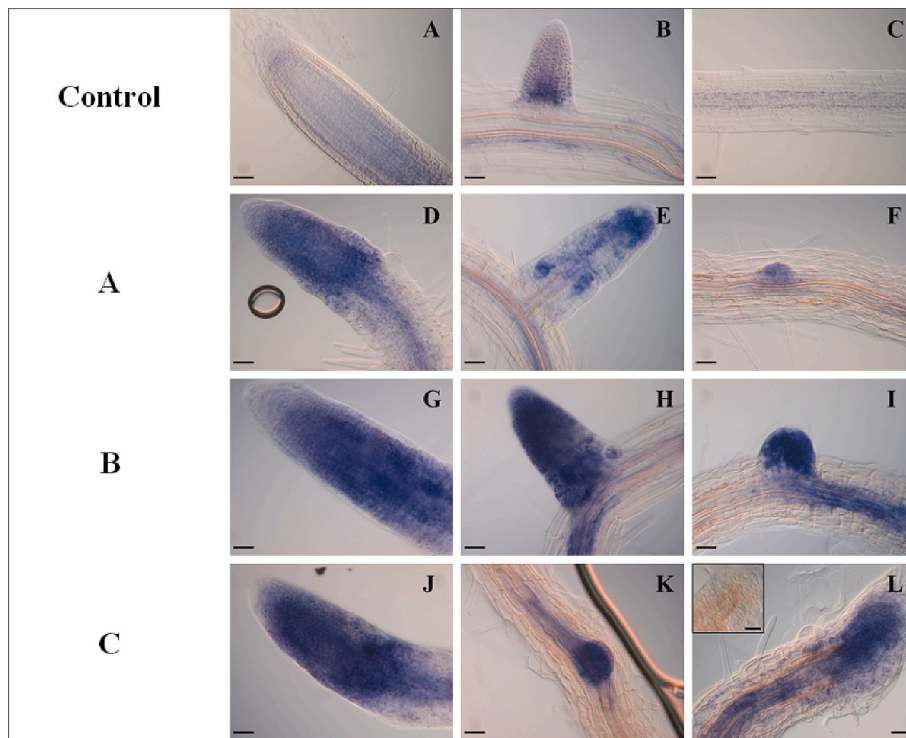
Fig. 8. Localization of superoxide anion ($\cdot O_2^-$) by NBT staining in the primary and secondary roots of *A. thaliana* seedlings grown for 14 days in the presence of the A, B and C PM$_{2.5}$ samples. In detail: Control (A, B, and C), sample A (D, E, and F), sample B (G, H, and I), sample C (J, K, and L). Bars = 40 μm. N = 5 per treatment.
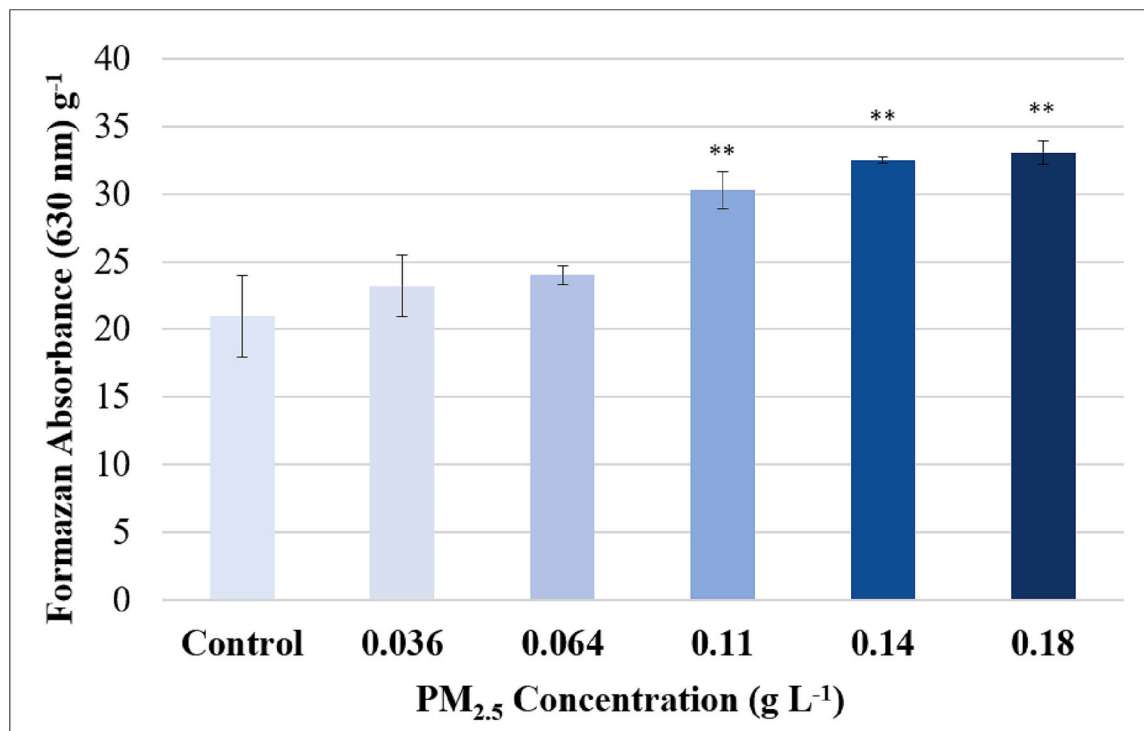

Fig. 9. Mean values (±SD) of formazan absorbance signal in *A. thaliana* exposed to 0.036, 0.064, 0.11, 0.14, and 0.18 g L^{-1} of PM$_{2.5}$; p-values of the paired-sample *t*-test between each treatment and Control: *** = p < 0.001; ** = p < 0.01; * = p < 0.05.

oxidative stress effects and localize $\cdot O_2^-$ production even in treatments with low PM mass concentrations, further optimizations of the method for the quantitative determination of $\cdot O_2^-$ as a biomarker of oxidative stress are needed to increase its sensitivity.

4. Conclusions

In this study, an innovative method for the assessment of the ability of PM to induce oxidative stress by in-vivo exposure of a model organism

was optimized and applied to samples of PM at different concentrations and with different chemical-physical properties. The results obtained show that *A. thaliana* can be an excellent plant model organism for the evaluation of the toxicological potential of PM. The assessment of the effects of oxidative stress using the NBT assay allowed the determination and localization of $\bullet O_2^-$ production in the seedlings exposed to PM. From the results obtained, it is evident that oxidative stress generation depends mainly on the concentration, chemical composition, and sources of the PM to which the seedlings are exposed. Particles released by biomass burning appeared to contribute more to the overall toxicity of PM; however, further studies are needed to identify significant relationships between the chemical-physical characteristics of PM and oxidative stress responses in *A. thaliana*. Finally, although the sensitivity of the method is rather low, it has been shown that this method is remarkably efficient in assessing the ability of PM to induce oxidative stress and that it provides statistically significant results when applied to single PM filters with relatively high PM mass concentrations (>20 µg m^{-3}). However, even at low concentrations, it is possible to study the formation of superoxide anion and thus the mechanisms of oxidative stress generation in the plant model organism by observing the roots of the seedlings exposed under an optical microscope. This method was found to be cost-effective and easy to apply to PM collected on membrane filters. We believe that this could be an effective approach to be applied in intensive PM monitoring campaigns for a thorough understanding of how PM generates oxidative damage and cytotoxic outcomes inside complete living organisms.

Further studies are needed, but the results presented here represent a first step toward the study of PM-induced effects through in-vivo exposure of model/experimental organisms.

Supplementary data to this article can be found online at https://doi.org/10.1016/j.scitotenv.2023.165694.

CRediT authorship contribution statement

Conceptualization: Diego Piacentini, Giuseppina Falasca, Silvia Canepari and Lorenzo Massimi; Data curation: Emanuele Vaccarella, Diego Piacentini and Lorenzo Massimi; Formal analysis: Emanuele Vaccarella, Diego Piacentini and Lorenzo Massimi; Supervision: Diego Piacentini, Giuseppina Falasca, Silvia Canepari and Lorenzo Massimi; Fundings: Giuseppina Falasca and Silvia Canepari; Writing – original draft: Emanuele Vaccarella; Writing – review & editing: Lorenzo Massimi.

Declaration of competing interest

The authors declare that they have no known competing financial interests or personal relationships that could have appeared to influence the work reported in this paper.

Data availability

Data will be made available on request.

Acknowledgments

References

Abozeid, A., Ying, Z., Lin, Y., Liu, J., Zhang, Z., Tang, Z., 2017. Ethylene improves root system development under cadmium stress by modulating superoxide anion concentration in Arabidopsis thaliana. Front. Plant Sci. 8, 253.

Alves, D.D., Riegel, R.P., Klauck, C.R., Ceratti, A.M., Hansen, J., Cansi, L.M., Osório, D.M. M., 2020. Source apportionment of metallic elements in urban atmospheric particulate matter and assessment of its water-soluble fraction toxicity. Environ. Sci. Pollut. Res. 27 (11), 12202–12214.

Bates, J.T., Fang, T., Verma, V., Zeng, L., Weber, R.J., Tolbert, P.E., Russell, A.G., 2019. Review of acellular assays of ambient particulate matter oxidative potential: methods and relationships with composition, sources, and health effects. Environ. Sci. Technol. 53 (8), 4003–4019.

Belis, C.A., Karagulian, F., Amato, F., Almeida, M., Artaxo, P., Beddows, D.C.S., Hopke, P. K., 2015. A new methodology to assess the performance and uncertainty of source apportionment models II: the results of two European intercomparison exercises. Atmos. Environ. 123, 240–250.

Canepari, S., Pietrodangelo, A., Perrino, C., Astolfi, M.L., Marzo, M.L., 2009. Enhancement of source traceability of atmospheric PM by elemental chemical fractionation. Atmos. Environ. 43 (31), 4754–4765.

Canepari, S., Astolfi, M.L., Farao, C., Maretto, M., Frasca, D., Marcoccia, M., Perrino, C., 2014. Seasonal variations in the chemical composition of particulate matter: a case study in the Po Valley. Part II: concentration and solubility of micro-and trace-elements. Environ. Sci. Pollut. Res. 21 (6), 4010–4022.

Canepari, S., Astolfi, M.L., Catrambone, M., Frasca, D., Marcoccia, M., Marcovecchio, F., Perrino, C., 2019. A combined chemical/size fractionation approach to study winter/summer variations, ageing and source strength of atmospheric particles. Environ. Pollut. 253, 19–28.

Celo, V., Yassine, M.M., Dabek-Zlotorzynska, E., 2021. Insights into elemental composition and sources of fine and coarse particulate matter in dense traffic areas in Toronto and Vancouver, Canada. Toxics 9 (10), 264.

Cho, U.H., Seo, N.H., 2005. Oxidative stress in Arabidopsis thaliana exposed to cadmium is due to hydrogen peroxide accumulation. Plant Sci. 168 (1), 113–120.

Chung, M.C., Tsai, M.H., Que, D.E., Bongo, S.J., Hsu, W.L., Tayo, L.L., Chao, H.R., 2019. Fine particulate matter-induced toxic effects in an animal model of caenorhabditis elegans. Aerosol Air Qual. Res. 19 (5), 1068–1078.

Classic Murashige, T., Skoog, F., 1962. A revised medium for rapid growth and bioassays with tobacco tissue cultures. Physiol. Plant 15, 473–497.

Costabile, F., Gualtieri, M., Canepari, S., Tranfo, G., Consales, C., Grollino, M.G., Simonetti, G., 2019. Evidence of association between aerosol properties and in-vitro cellular oxidative response to PM1, oxidative potential of PM2. 5, a biomarker of RNA oxidation, and its dependency on combustion sources. Atmos. Environ. 213, 444–455.

Costantini, D., 2019. Understanding diversity in oxidative status and oxidative stress: the opportunities and challenges ahead. J. Exp. Biol. 222 (13), jeb194688.

Crobeddu, B., Aragao-Santiago, L., Bui, L.C., Boland, S., Squiban, A.B., 2017. Oxidative potential of particulate matter 2.5 as predictive indicator of cellular stress. Environ. Pollut. 230, 125–133.

Daellenbach, K.R., Uzu, G., Jiang, J., Cassagnes, L.E., Leni, Z., Vlachou, A., Prévôt, A.S., 2020. Sources of particulate-matter air pollution and its oxidative potential in Europe. Nature 587 (7834), 414–419.

de Santana, Verçosa, C.J., de Araújo Castro, de Amorim, da Silva, da Rocha Bastos, Rohde, C., 2018. Drosophila melanogaster as model organism for monitoring and analyzing genotoxicity associated with city air pollution. Environ. Sci. Pollut. Res. 25, 32409–32417.

Demecsová, L., Zelinová, V., Liptáková, Ľ., Valentovićová, K., Tamás, L., 2020. Indole-3-butyric acid priming reduced cadmium toxicity in barley root tip via NO generation and enhanced glutathione peroxidase activity. Planta 252 (3), 1–16.

Duan, J., Hu, H., Zhang, Y., Feng, L., Shi, Y., Miller, M.R., Sun, Z., 2017. Multi-organ toxicity induced by fine particulate matter PM2. 5 in zebrafish (Danio rerio) model. Chemosphere 180, 24–32.

Farooq, M.A., Islam, F., Ali, B., Najeeb, U., Mao, B., Gill, R.A., Zhou, W., 2016. Arsenic toxicity in plants: cellular and molecular mechanisms of its transport and metabolism. Environ. Exp. Bot. 132, 42–52.

Fattorini, L., Ronzan, M., Piacentini, D., Della Rovere, F., De Virgilio, C., Sofo, A., Altamura, M.M., Falasca, G., 2017. Cadmium and arsenic affect quiescent centre formation and maintenance in Arabidopsis thaliana post-embryonic roots disrupting auxin biosynthesis and trasport. Environ. Exp. Bot. 144, 37–48.

Ficociello, G., Inverni, A., Massimi, L., Buccini, G., Canepari, S., Uccelletti, D., 2020. Assessment of the effects of atmospheric pollutants using the animal model Caenorhabditis elegans. Environ. Res. 191, 110209.

Frezzini, M.A., De Francesco, N., Massimi, L., Canepari, S., 2022a. Effects of operating conditions on PM oxidative potential assays. Atmos. Environ. 268, 118802.

Frezzini, M.A., Di Iulio, G., Tiraboschi, C., Canepari, S., Massimi, L., 2022b. A new method for the assessment of the oxidative potential of both water-soluble and insoluble PM. Atmosphere 13 (2), 349.

Gualtieri, M., Grollino, M.G., Consales, C., Costabile, F., Manigrasso, M., Avino, P., Zanini, G., 2018. Is it the time to study air pollution effects under environmental conditions? A case study to support the shift of in vitro toxicology from the bench to the field. Chemosphere 207, 552–564.

Guo, J., Dai, X., Xu, W., Ma, M., 2008. Overexpressing GSH1 and AsPCS1 simultaneously increases the tolerance and accumulation of cadmium and arsenic in Arabidopsis thaliana. Chemosphere 72 (7), 1020–1026.

Haider, F.U., Liqun, C., Coulter, J.A., Cheema, S.A., Wu, J., Zhang, R., Farooq, M., 2021. Cadmium toxicity in plants: impacts and remediation strategies. Ecotoxicol. Environ. Saf. 211, 111887.

Inskeep, W.P., Bloom, P.R., 1985. Extinction coefficients of chlorophyll a and b in N, N-dimethylformamide and 80% acetone. Plant Physiol. 77 (2), 483–485.

Lavigne, É., Talarico, R., van Donkelaar, A., Martin, R.V., Stieb, D.M., Crighton, E., Chen, H., 2021. Fine particulate matter concentration and composition and the incidence of childhood asthma. Environ. Int. 152, 106486.

Lionetto, M.G., Guascito, M.R., Giordano, M.E., Caricato, R., De Bartolomeo, A.R., Romano, M.P., Contini, D., 2021. Oxidative potential, cytotoxicity, and intracellular oxidative stress generating capacity of PM10: a case study in south of Italy. Atmosphere 12 (4), 464.

Loomis, D., Grosse, Y., Lauby-Secretan, B., Ghissassi, F.E., Bouvard, V., Benbrahim-Tallaa, L., Guha, N., Baan, R., Mattock, H., Straif, K., International Agency for Research on Cancer Monograph Working Group IARC, 2013. The carcinogenicity of outdoor air pollution. Lancet Oncol. 14, 1262–1263.

Manjunatha, B., Deekshitha, B., Seo, E., Kim, J., Lee, S.J., 2021. Developmental toxicity induced by particulate matter (PM2. 5) in zebrafish (Danio rerio) model. Aquat. Toxicol. 238, 105928.

Marchetti, S., Hassan, S.K., Shetaya, W.H., El-Mekawy, A., Mohamed, E.F., Mohammed, A.M., Mantecca, P., 2019. Seasonal variation in the biological effects of PM2. 5 from greater Cairo. Int. J. Mol. Sci. 20 (20), 4970.

Marcoccia, M., Ronci, L., De Matthaeis, E., Setini, A., Perrino, C., Canepari, S., 2017. In-vivo assesment of the genotoxic and oxidative stress effects of particulate matter on Echinogammarus veneris. Chemosphere 173, 124–134.

Martin, P.J., Heliot, A., Tremolet, G., Landkocz, Y., Dewaele, D., Cazier, F., Courcot, D., 2019. Cellular response and extracellular vesicles characterization of human macrophages exposed to fine atmospheric particulate matter. Environ. Pollut. 254, 112933.

Massimi, L., Simonetti, G., Buiarelli, F., Di Filippo, P., Pomata, D., Riccardi, C., Canepari, S., 2020a. Spatial distribution of levoglucosan and alternative biomass burning tracers in atmospheric aerosols, in an urban and industrial hot-spot of Central Italy. Atmos. Res. 239, 104904.

Massimi, L., Ristorini, M., Simonetti, G., Frezzini, M.A., Astolfi, M.L., Canepari, S., 2020b. Spatial mapping and size distribution of oxidative potential of particulate matter released by spatially disaggregated sources. Environ. Pollut. 266, 115271.

Massimi, L., Pietrodangelo, A., Frezzini, M.A., Ristorini, M., De Francesco, N., Sargolini, T., Perrino, C., 2022a. Effects of COVID-19 lockdown on PM10 composition and sources in the Rome Area (Italy) by elements' chemical fractionation-based source apportionment. Atmos. Res. 266, 105970.

Massimi, L., Astolfi, M.L., Canepari, S., 2022b. Simple and efficient method to detach intact PM10 from field filters: elements recovery assessment. Atmos. Pollut. Res. 101871.

Mirowsky, J.E., Jin, L., Thurston, G., Lighthall, D., Tyner, T., Horton, L., Gordon, T., 2015. In vitro and in vivo toxicity of urban and rural particulate matter from California. Atmos. Environ. 103, 256–262.

Molina, C., Toro, A.R., Manzano, C.A., Canepari, S., Massimi, L., Leiva-Guzmán, M., 2020. Airborne aerosols and human health: leapfrogging from mass concentration to oxidative potential. Atmosphere 11 (9), 917.

Mooibroek, D., Sofowote, U.M., Hopke, P.K., 2022. Source apportionment of ambient PM10 collected at three sites in an urban-industrial area with multi-time resolution factor analyses. Sci. Total Environ. 157981.

Øvrevik, J., 2019. Oxidative potential versus biological effects: a review on the relevance of cell-free/abiotic assays as predictors of toxicity from airborne particulate matter. Int. J. Mol. Sci. 20 (19), 4772.

Palleschi, S., Rossi, B., Armiento, G., Montereali, M.R., Nardi, E., Tagliani, S.M., Silvestroni, L., 2018. Toxicity of the readily leachable fraction of urban PM2. 5 to human lung epithelial cells: role of soluble metals. Chemosphere 196, 35–44.

Pant, P., Harrison, R.M., 2013. Estimation of the contribution of road traffic emissions to particulate matter concentrations from field measurements: a review. Atmos. Environ. 77, 78–97.

Peixoto, M.S., de Oliveira Galvão, M.F., de Medeiros, S.R.B., 2017. Cell death pathways of particulate matter toxicity. Chemosphere 188, 32–48.

Perrino, C., Canepari, S., Pappalardo, S., Marconi, E., 2010. Time-resolved measurements of water-soluble ions and elements in atmospheric particulate matter for the characterization of local and long-range transport events. Chemosphere 80 (11), 1291–1300.

Perrino, C., Catrambone, M., Dalla Torre, S., Rantica, E., Sargolini, T., Canepari, S., 2014. Seasonal variations in the chemical composition of particulate matter: a case study in the Po Valley. Part I: macro-components and mass closure. Environ. Sci. Pollut. Res. 21 (6), 3999–4009.

Piacentini, D., Falasca, G., Canepari, S., Massimi, L., 2019. Potential of PM-selected components to induce oxidative stress and root system alteration in a plant model organism. Environ. Int. 132, 105094.

Piacentini, D., Corpas, F.J., D'Angeli, S., Altamura, M.M., Falasca, G., 2020. Cadmium and arsenic-induced-stress differentially modulates Arabidopsis root architecture, peroxisome distribution, enzymatic activities and their nitric oxide content. Plant Physiol. Biochem. 148, 312–323.

Piacentini, D., Della Rovere, F., Bertoldi, I., Massimi, L., Sofo, A., Altamura, M.M., Falasca, G., 2021. Peroxisomal PEX7 receptor affects cadmium-induced ROS and auxin homeostasis in Arabidopsis root system. Antioxidants 10 (9), 1494.

Ramírez, O., de la Campa, Sánchez-Rodas, D., de la Rosa, J.D., 2020. Hazardous trace elements in thoracic fraction of airborne particulate matter: assessment of temporal variations, sources, and health risks in a megacity. Sci. Total Environ. 710, 136344.

Romani, A., Cervellati, C., Muresan, X.M., Belmonte, G., Pecorelli, A., Cervellati, F., Valacchi, G., 2018. Keratinocytes oxidative damage mechanisms related to airborne particle matter exposure. Mech. Ageing Dev. 172, 86–95.

Saggu, G.S., Mittal, S.K., 2020. Source apportionment of PM10 by positive matrix factorization model at a source region of biomass burning. J. Environ. Manag. 266, 110545.

Simonetti, G., Conte, E., Perrino, C., Canepari, S., 2018. Oxidative potential of size-segregated PM in an urban and an industrial area of Italy. Atmos. Environ. 187, 292–300.

Williams, R., Suggs, J., Rea, A., Leovic, K., Vette, A., Croghan, C., Sanders Jr., W., 2003. The Research Triangle Park particulate matter panel study: PM mass concentration relationships. Atmos. Environ. 37 (38), 5349–5363.

World Health Organization, 2016. Ambient Air Pollution: A Global Assessment of Exposure and Burden of Diseases.

Zhang, Y., Li, Z., 2015. Remote sensing of atmospheric fine particulate matter (PM2. 5) mass concentration near the ground from satellite observation. Remote Sens. Environ. 160, 252–262.

Zhou, X., Xiang, Y., Li, C., Yu, G., 2020. Modulatory role of reactive oxygen species in root development in model plant of Arabidopsis thaliana. Front. Plant Sci. 11, 485932.

Zwiewka, M., Bielach, A., Tamizhselvan, P., Madhavan, S., Ryad, E.E., Tan, S., Tognetti, V.B., 2019. Root adaptation to H_2O_2-induced oxidative stress by ARF-GEF BEN1-and cytoskeleton-mediated PIN2 trafficking. Plant Cell Physiol. 60 (2), 255–273.